

Boundary-layer dynamics and its influence on atmospheric chemistry at Summit, Greenland

Lana Cohen^a, Detlev Helmig^{a,*}, William D. Neff^b,
Andrey A. Grachev^c, Christopher W. Fairall^b

^a*Institute of Arctic and Alpine Research, University of Colorado at Boulder, UCB 450, Boulder, CO 80309, USA*

^b*NOAA Earth System Research Laboratory, Physical Sciences Division, 325 Broadway, Boulder, CO 80305, USA*

^c*Cooperative Institute for Research in Environmental Sciences, University of Colorado and NOAA Earth System Research Laboratory, Physical Sciences Division, 325 Broadway, Boulder, CO 80305, USA*

Received 15 September 2005; received in revised form 20 June 2006; accepted 29 June 2006

Abstract

Sonic anemometer turbulence measurements were made at Summit, Greenland during summer 2004 and spring 2005. These measurements allow for the characterization of the variability of the atmospheric boundary layer at this site by describing seasonal and diurnal changes in sensible heat flux and boundary layer stability as well as providing estimates of mixing layer height. Diurnal sensible heat fluxes at Summit ranged from -18 to -2 W m^{-2} in the spring and from -7 to $+10 \text{ W m}^{-2}$ in the summer. Sustained stable surface layer conditions and low wind speeds occurred during the spring but not during the summer months. Unstable conditions were not observed at Summit until late April. Diurnal cycles of convective conditions during the daytime (0700–1700 h local time) were observed throughout July and August. Boundary layer heights, which were estimated for neutral to stable conditions, averaged 156 m for the spring 2005 observations. Comparisons of the boundary layer characteristics of Summit with those from South Pole, Antarctica, provide possible explanations for the significant differences in snowpack and surface-layer chemistry between the two sites.

© 2007 Published by Elsevier Ltd.

Keywords: Polar boundary layer; Seasonal changes; Surface-atmosphere fluxes; Surface layer chemistry

1. Introduction

An emphasis of recent polar atmospheric research has been the study of snow-photochemical processes and their influence on surface and boundary layer chemistry. It is becoming increasingly evident that trace contaminants in sunlit snow are the source for

vigorous chemical activity within the snow and in the atmospheric surface layer. Several trace gas species, which have been identified among the myriad of reactants that are involved in these chemical reaction cycles, play a critical role in determining the oxidation capacity of air. Since interstitial air readily exchanges with the atmosphere above the snowpack by diffusion and wind-driven ventilation, reactions in the snowpack constitute both sources and sinks for reactive trace

*Corresponding author. Tel.: +1 303 492 2509.

E-mail address: Detlev.Helmig@colorado.edu (D. Helmig).

gases in the polar surface and boundary layer. Of particular importance for the oxidation chemistry in the polar atmosphere are the fluxes and budgets of oxidized nitrogen species, hydrogen peroxide and carbonyl compounds, as these short-lived gases determine the cycling of HO_x and RO_x radicals and the oxidation chemistry in the surface layer. The significant snowpack-to-atmosphere fluxes of oxidant precursor compounds result in unexpectedly high concentrations of OH_x and RO_x in the polar surface layer. Ambient mixing ratios of oxidized nitrogen species at South Pole were found to approach and occasionally exceed the 1 ppbv level during summertime conditions (Davis et al., 2001, 2004). Hydroxyl and OH+RO₂ radicals at South Pole were highly elevated, with mean values of 2.5×10^6 and 7×10^7 molecule cm⁻³ during November and December (Mauldin et al., 2004).

Studies at South Pole (ISCAT 1998, ISCAT 2000, ANTCD) have been paralleled by research at Arctic sites, including Alert, Nunavut, Canada, and Summit, Greenland (Bottenheim et al., 2002 and references therein). While many similarities in the snowpack physics and chemistry between these sites have been discovered, surface and boundary layer concentrations and chemistry of trace gases were found to differ substantially. The most important, contrasting finding is that concentrations of nitrogen oxides (NO_x) at South Pole reach levels approximately a factor of ten higher than at Summit (Honrath et al., 2002; Davis et al., 2004). This substantial enhancement of NO_x in the South Pole surface layer is expected to result in significant photochemical ozone production (Crawford et al., 2001). The model calculations by Crawford et al. were subsequently confirmed by high resolution vertical ozone gradient measurements: Ozone enhancements of up to 25 ppbv were found to frequently occur in the South Pole surface layer during the Austral summer (Helmig et al. 2007a; Oltmans et al., 2007). Episodes with elevated ozone persisted for extended periods (4–5 days) and were correlated with stable atmospheric boundary layer conditions. In contrast, a recent investigation of the ozone chemistry in Greenland concluded that surface layer ozone production is of much lower importance at Summit (Helmig et al., 2007b).

Since snowpack photochemistry and snow-atmosphere gas exchange fluxes do not appear to differ that much between these two sites, it is plausible that boundary-layer dynamics play an important role in determining the differences in the accumulation and

photochemical equilibrium of reactive trace gases in the surface and boundary layer between Summit and South Pole. Therefore, during several recent campaigns at Summit and South Pole, turbulence, sodar soundings, radiosonde, tethered balloon and tower gradient instruments were deployed in order to develop a better understanding of the dependency of surface layer chemistry on boundary layer mixing and transport processes. In this manuscript we present data and interpretations from two experiments at Summit that used turbulence, tethered balloon, and tower gradient measurements. While these data are the primary focus of the manuscripts, they are also contrasted with similar observations at the South Pole (Neff et al., 2007), a similarly high (2835 m), flat, and dry snow zone site on the Antarctic plateau. In particular, Davis et al. (2004) hypothesized that the extremely high NO concentrations observed at the South Pole could be explained by the presence of a very thin boundary layer and long fetches for air flow off the high Antarctic plateau. Using sodar measurements, Neff et al. (2007) confirmed that such thin boundary layers did exist at the South Pole. These researchers also evaluated a simple mixing height estimation method for stable conditions that uses surface turbulence parameters and vertical stability. Of importance in our analysis is the extent to which their results are transferable to the Summit site, particularly in light of a significantly shorter fetch and the presence of a significant diurnal solar radiation cycle.

2. Instrumentation and methods

2.1. Turbulence measurements

Turbulence measurements with a sonic anemometer were carried out at Summit (72°34'N, 38°29'W, elevation 3212 m) (Fig. 1) throughout two periods during 2004 and 2005. Sonic turbulence data were collected for 48 consecutive days during the summer 2004 field season between 27 June and 14 August (day of year (DOY) 178–226) and for 51 days during 2005 between 8 March and 28 April (DOY 67–118). The sonic anemometer (Campbell Scientific CSAT3) was installed on the 'Science Tower' which is located ~250 m south (upwind) of camp structures in the Summit 'Clean Air Zone'. The sonic anemometer was mounted 2 m above the snow surface and connected to a data acquisition system located in the 'Science Trench' approximately 10 m under the snow surface beneath the tower.

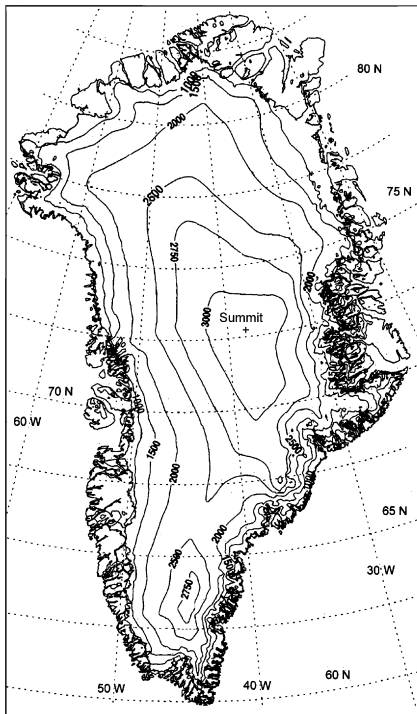


Fig. 1. Location of Summit and topography of Greenland ice sheet (map courtesy of the Steffen Research group: <http://cires.colorado.edu/steffen/>).

Data were collected at sampling rates of 25 Hz for the first 6 days (DOY 178–184) of the 2004 period, then at 60 Hz averaged to 20 Hz for the rest of the 2004 period, and at 48 Hz averaged to 16 Hz during the 2005 experiment.

The sonic anemometer provided measurements of the three wind components (streamwise, u ; cross-stream, v ; and vertical, w) and sonic temperature (T_s). Turbulent covariance values ($\overline{u'w'}$, $\overline{v'w'}$, $\overline{w'T'_s}$) were derived via eddy-correlation based on $\frac{1}{2}$ -h averaging. The overbars indicate a time averaging operator and ($'$) denotes fluctuation about the mean value, e.g., $u = \bar{u} + u'$. The sonic anemometer also provided measurements of the mean wind speed vector (magnitude and direction).

Rotation of the anemometer coordinate system was applied to place the anemometer in the streamwise coordinate system. This rotation sets $\bar{v} = 0$. A second rotation of the coordinate system sets $\bar{w} = 0$. Momentum flux (τ) and sensible heat flux (H_s) were derived from the measured covariance values according to

$$\tau = \rho u_*^2 = -\rho \overline{u'w'}, \quad (1)$$

and

$$H_s = c_p \rho \overline{w'T'}, \quad (2)$$

where u_* is the friction velocity, ρ is air density, T is the air temperature, and c_p is the heat capacity of air at constant pressure.

The sonic anemometer measures the so-called ‘sonic’ virtual temperature, T_s , which is close to the virtual temperature used in calculating kinematic heat flux, $w'T'$, and the sensible heat flux, H_s . That is, the temperature derived from the speed of sound measurements (sonic temperature), $T_s = T(1 + 0.51q)$ (where q is the water vapor mixing ratio), has the same form as the virtual temperature $T_v = T(1 + 0.61q)$ (e.g. Kaimal and Gaynor, 1991; Larsen et al., 1993; Kaimal and Finnigan, 1994), and often T_s is referred to simply as the virtual temperature. The error involved in assuming $T_s \approx T_v$ is on the order of 0.01° (Kaimal and Gaynor, 1991). The associated error in not correcting the kinematic temperature flux (and thus the sensible heat flux) for specific humidity (q) is especially low in polar, dry snow conditions. The moisture correction for using the sonic temperature instead of the virtual temperature is $\overline{w'T'} = \overline{w'T'_s} - 0.51T\overline{w'q} \approx \overline{w'T'_s} / (1 + 0.06/Bo)$, (Andreas and Cash, 1996), where the Bowen ratio, $Bo = H_s/H_L$, is the ratio of sensible heat flux to latent heat flux. Based on monthly averages of latent and sensible heat fluxes at Summit (Cullen, 2003), the Bowen ratio in spring and summer ranges between 1 and 3. This implies an error in overestimation of sensible heat flux from 2% to 6%.

Turbulence data were processed in $\frac{1}{2}$ -h blocks (36,000 data points for 20 Hz data, 28,800 for 16 Hz data). A despiking procedure eliminated raw data outliers. Fourier transform segments were selected for calculating variances and covariances such that each ‘‘half-hour’’ value is actually calculated from the first 2^{14} points (17.1 min) for 16 Hz data and 2^{15} points (27.3 min) for 20 Hz data. Hamming window and linear detrending was applied to each data block before calculating spectral and cospectral densities. Spectra and cospectra were then smoothed such that the frequency interval expands with frequency. Fluxes for each $\frac{1}{2}$ h were determined by integrating cospectra of the proper variables (i.e. integration of wT cospectra yields $\overline{w'T'}$ covariance) over frequencies from 0.1 s to 27.3 min for 20 Hz and from 0.26 s to 17.1 min for 16 Hz.

Frequency-weighted spectra (u , v , w , and T) and cospectra (uw , vw , and wT) for each $\frac{1}{2}$ -h run were

plotted against frequency and used to determine data quality. Only runs which exhibited the spectral characteristics of Monin–Obukhov similarity theory (MOST), e.g. a $-\frac{2}{3}$ slope in the inertial subrange (falling portion of the spectral curve) were kept for calculating fluxes (see Fig. 2). Runs which did not exhibit MOST were primarily attributed to tower interference (wind coming through the tower before reaching the sonic transducers), intermittent turbulence (occurring in very stable, calm surface layer conditions), and nonstationarity (significant boundary layer changes within the $\frac{1}{2}$ -h period). Rime, heavy snow, and extremely cold temperatures (below -38°C), which caused instrument malfunction, were also reasons for data losses. There were also several periods of data loss due to computer and/or datalogger malfunctions. The total number of useable runs was 62% during 2004 and 46% for the 2005 period. In 2004, 9% of data were lost due to flow distortion (wind direction between 250° and 290°) and 0% were lost due to low temperatures. In 2005, 7.5% of data were lost due to flow distortion and 28% were lost due to temperature extremes. The rest of the unusable data (53% for 2004; 11% for 2005) can be attributed to nonstationarity. Cullen (2003) also found that 40% of his turbulence data during mid-summer conditions was unusable for reasons of nonstationarity. Inspection of individual as well as averaged spectra and cospectra plots from the 2005 data show “tails” in the high frequencies that indicate some problems with the data. The noise in the high frequency range is most likely indicative of electronic interference (Kaimal and Finnigan, 1994). Thus, the 2005 fluxes were calculated omitting frequencies greater than 3.91 Hz.

Figs. 2 and 3 show average spectra and cospectra for all useable runs during 2004 and 2005. The spectra all have a slope of $-\frac{2}{3}$ in the inertial subrange in these coordinates. During the summer 2004 period, the spectra and cospectra are not separated for stable and unstable conditions (negative and positive kinematic heat fluxes, $w'T'$), as can be seen from the near-zero wT cospectra (Fig. 3a) indicating minor sensible heat fluxes in the summer. For the springtime, stable boundary layer cospectra (Fig. 3b), note that the negative wT cospectral peak is well-identified and shifted to the right of the uw peak, indicating that heat is transported downward more efficiently at higher frequencies as discussed by Kaimal and Finnigan (1994). These results reveal the significant differences between spring and summer turbulence regimes.

2.2. Tower gradient measurements

In addition to the sonic anemometer turbulence data, temperature and wind speed gradient data were necessary to estimate boundary layer heights. The required tower measurements were collected during the 2004 field season at the Science Trench Tower at heights of 0.5, 2 and 10 m. The Science Tower instrumentation is described in detail by Helmig et al. (2007c). For the spring 2005 period, temperature and wind speed profile measurements were collected by the Swiss Federal Institute of Technology, Institute for Atmospheric and Climate Science (ETH) at heights of 0.5, 1.5, 4.5 and 5.5 m. The Swiss Tower instruments are located ~ 200 m east–northeast of the Science Trench Tower.

2.3. Radiosonde soundings

NOAA’s Global Monitoring Division (GMD) launched 20 ozonesondes at Summit during the spring 2005 observation period. Vertical profiles of ozone concentration, ambient pressure, temperature and relative humidity were measured from the balloon-borne ozonesondes with an integrated Vaisala Model RS80-15 radiosonde for data telemetry to the ground receiving station.

3. Results and discussion

3.1. Surface layer conditions

Atmospheric surface layer conditions contrast greatly between the summer 2004 and spring 2005 measurement periods and are summarized in Table 1. The mean virtual temperature as measured by the sonic anemometer (30-min averages) for July and August 2004 was -12.5°C with a standard deviation of 4.6°C , and for March–April 2005 was -25.1°C with a standard deviation of 6.3°C . Wind speeds also differed with winds greater during the spring season than during the summer (mean 7.3 m s^{-1} in the spring versus mean 4.2 m s^{-1} during the summer).

Wind directions were found to be primarily from the SE to SW directions with 97% of March–April 2005 winds between 90 – 270° and 78% of July–August 2004 winds between 90 – 270° , which is typical for Summit conditions (Stearns et al., 1997; Steffen and Box, 2001; Cullen, 2003). At Summit, large scale synoptic circulation and the influence of orographic flow around the Greenland ice cap is the

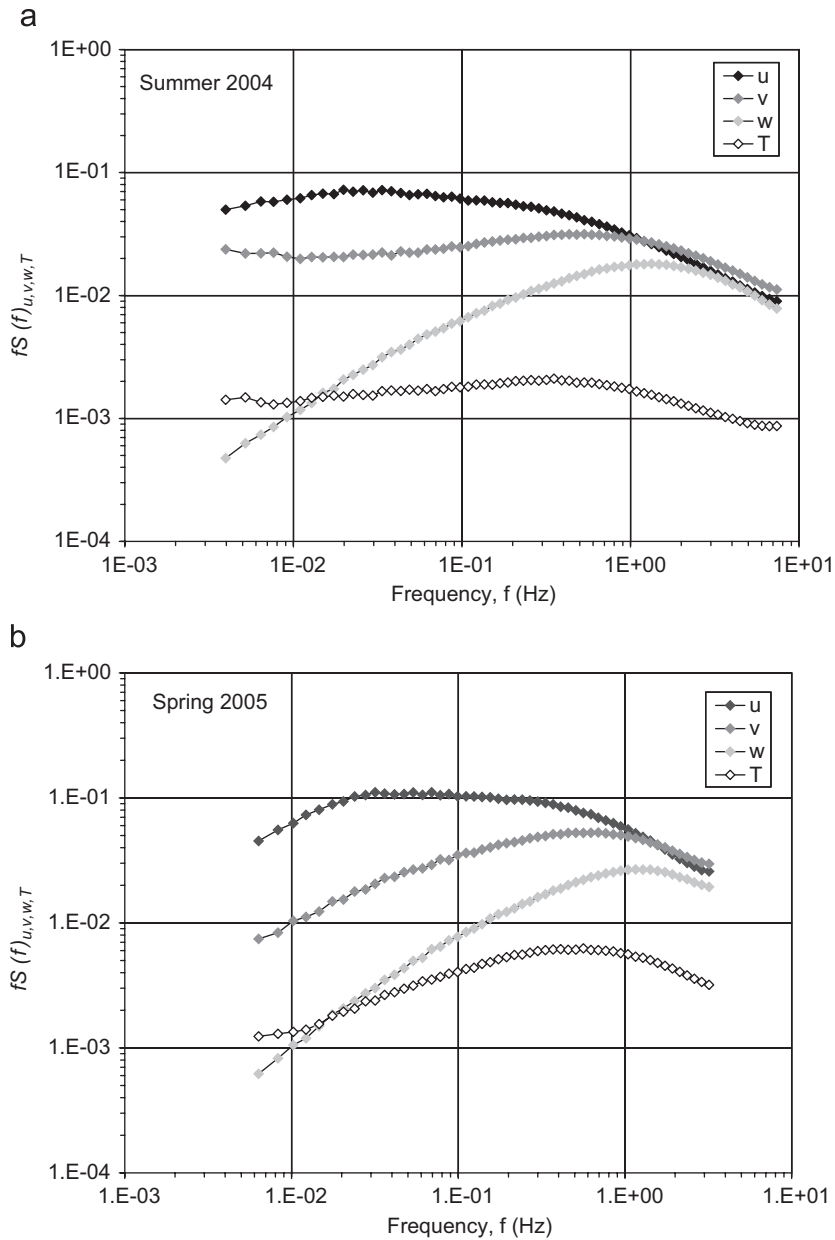


Fig. 2. Summer 2004 (upper graph, a) and spring 2005 (lower graph, b) surface layer u, v, w , and T spectra, where each spectrum $S(f)$ (of u, v, w, T) has been multiplied by the frequency f so that the integral of the area under the curve is the variance. Spectra are averages of all runs during each experimental period (1250 and 1112 runs respectively).

primary factor in determining the wind direction (Stearns et al., 1997; Steffen and Box, 2001). The observed seasonal differences in Summit surface conditions reflect the seasonal differences in boundary layer conditions which are discussed below.

Monin–Obukhov similarity theory, or surface-layer scaling, is the commonly accepted approach to

describe the near-surface atmospheric layer. According to MOST, properly scaled dimensionless characteristics of the turbulence at reference height z are universal functions of a stability parameter, z/L , where

$$L = - \frac{u_*^3 T_v}{\kappa g w' T'_v} \tag{3}$$

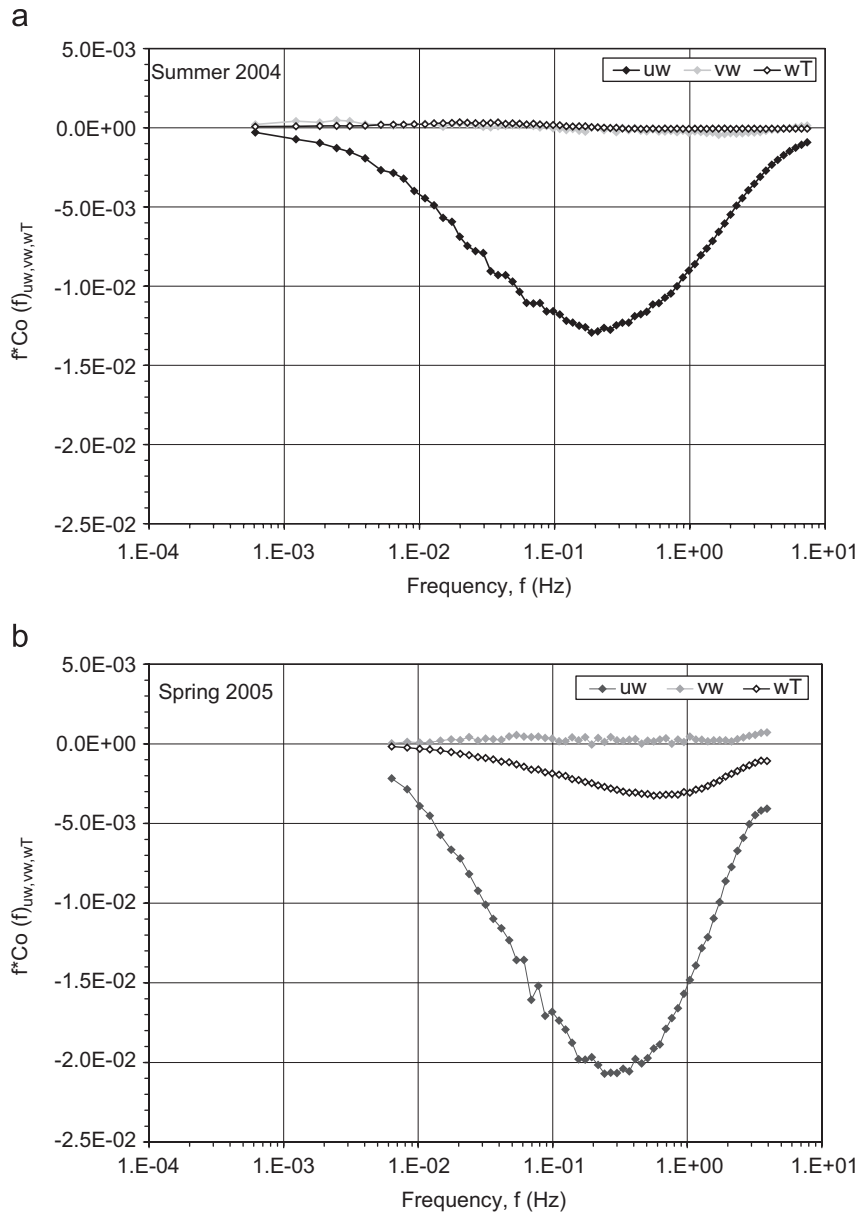


Fig. 3. Summer 2004 (upper graph, a) and spring 2005 (lower graph, b) surface layer uw , vw , and wT cospectra. Cospectra are averages of all runs during each experimental period (1250 and 1112 runs respectively).

is the Obukhov length (κ is the von Karman constant, and g is the acceleration due to gravity) (Kaimal and Finnigan, 1994). The friction velocity in Eq. (3) is computed according to Eq. (1). It should be noted that Eq. (3) is based on the measured fluxes of momentum and buoyancy in a thin surface layer where the fluxes are assumed to be constant with height.

Surface-layer parameters friction velocity (u_*) and the stability parameter (z/L) are also important for

describing surface layer conditions and are summarized in Table 1. The stability of the surface layer is expressed by the stability parameter, where z/L is positive for stable conditions and negative for unstable conditions (Kaimal and Finnigan, 1994).

Comparisons of the differences in wind regimes between Summit and South Pole, illuminate significant differences in the boundary layer behavior. Figs. 4a and b show mean half-hour wind speeds from sonic anemometer data for both Summit and

Table 1
Surface layer conditions at Summit during two experiments

	July–August 2004		March–April 2005	
	Mean	Standard deviation	Mean	Standard deviation
Virtual temperature (°C)	−12.5	4.64	−25.1	6.32
Wind speed (m s^{-1})	4.2	2.27	7.3	3.02
Friction velocity u_* (m s^{-1})	0.186	0.099	0.261	0.124
z/L	0.053	0.370	0.110	0.242

South Pole summers (Summit: July–August, 2004; South Pole: December 2003). The South Pole turbulence data analysis procedure was the same as that for Summit data (Neff et al., 2007). Of note are the more variable wind speed and lack of sustained calm conditions at Summit, which are in contrast to the extended period of low wind speeds ($\leq 2 \text{ m s}^{-1}$) at South Pole observed during DOY 355–358. For both Summit and South Pole, weak winds comprise 22% of the summer observation periods but light winds at Summit are much more intermittent. Table 2 summarizes the occurrences of weak wind conditions ($\leq 2 \text{ m s}^{-1}$ at 2 m above ground) for the spring and summer experiments at Summit and for the summer experiment at South Pole. The wind speed record for Summit has been supplemented with tower measurements at 2 m to fill gaps in the sonic data time series. At Summit, the longest stretch of $\leq 2 \text{ m s}^{-1}$ wind speeds occurring during the summer was 15 h (DOY 210.8–211.4) and during the spring was 30.5 h (DOY 100.6–101.85), whereas South Pole experienced a continuous 73 h (December day 21.60–24.65) of $\leq 2 \text{ m s}^{-1}$ wind speeds.

3.2. Heat fluxes

Sensible heat flux has been shown to be the largest component of net turbulent heat flux for Summit (Albert and Hawley, 2000; Cullen and Steffen, 2001). Fig. 5 shows the turbulent sensible heat fluxes calculated from sonic anemometer data for the summer 2004 and spring 2005 experiments. In the spring, the heat flux average is -11 W m^{-2} with a maximum of $+22 \text{ W m}^{-2}$ and a minimum of -39 W m^{-2} , while in the summer the heat flux average is $+1 \text{ W m}^{-2}$ with a maximum of $+35 \text{ W m}^{-2}$ and minimum of -33 W m^{-2} .

Negative sensible heat flux indicates heat flow towards the ground surface and stable surface layer conditions, whereas positive sensible heat flux

indicates heat flow away from the surface and unstable surface layer conditions. The differences seen in the two heat flux data series reflect the seasonal variation of net radiation flux and surface energy balance on the ice sheet. The large day-to-day variations seen during both periods most likely reveal changes in cloud-cover conditions and wind speeds due to synoptic variability. Averaging the turbulent heat flux values for each hour of the diurnal cycle (Fig. 6) reveals a significant seasonal difference. In the spring, the hourly averaged heat flux is never positive, while in the summer, the heat fluxes do become positive during the day.

Breaking down the seasonal heat fluxes into weekly averages shows the seasonal evolution in greater detail. In Fig. 7, weeks 11 (22–28 March) through 16 (15–27 April) encompass the 2005 observations, while weeks 26 (27 June–3 July) through 32 (12–18 August) cover the 2004 observations. The overall heat flux values can be seen to increase with time and become positive during the last weeks of the spring 2005 observation period (15–27 April). Weeks 26 to 32 show positive heat fluxes during the daytime between the hours of 0900 and 2000 h GMT (0700–1800 h local time). Cullen and Steffen (2001) also reported a similar diurnal cycle of heat fluxes during June and July at Summit.

Examination of the same analysis of turbulent data from South Pole (December 2003) shows sensible heat fluxes of a similar magnitude to those at Summit (average -0.25 W m^{-2}) but without a diurnal cycle (Neff et al., 2007). Sensible heat fluxes during the summer at South Pole demonstrate less temporal variation and can exhibit small, negative (downward) values under light wind conditions for several days at a time.

3.3. Stability in the surface layer

Fig. 8 illustrates an evolution of surface layer stability conditions as seen in the stability parameter

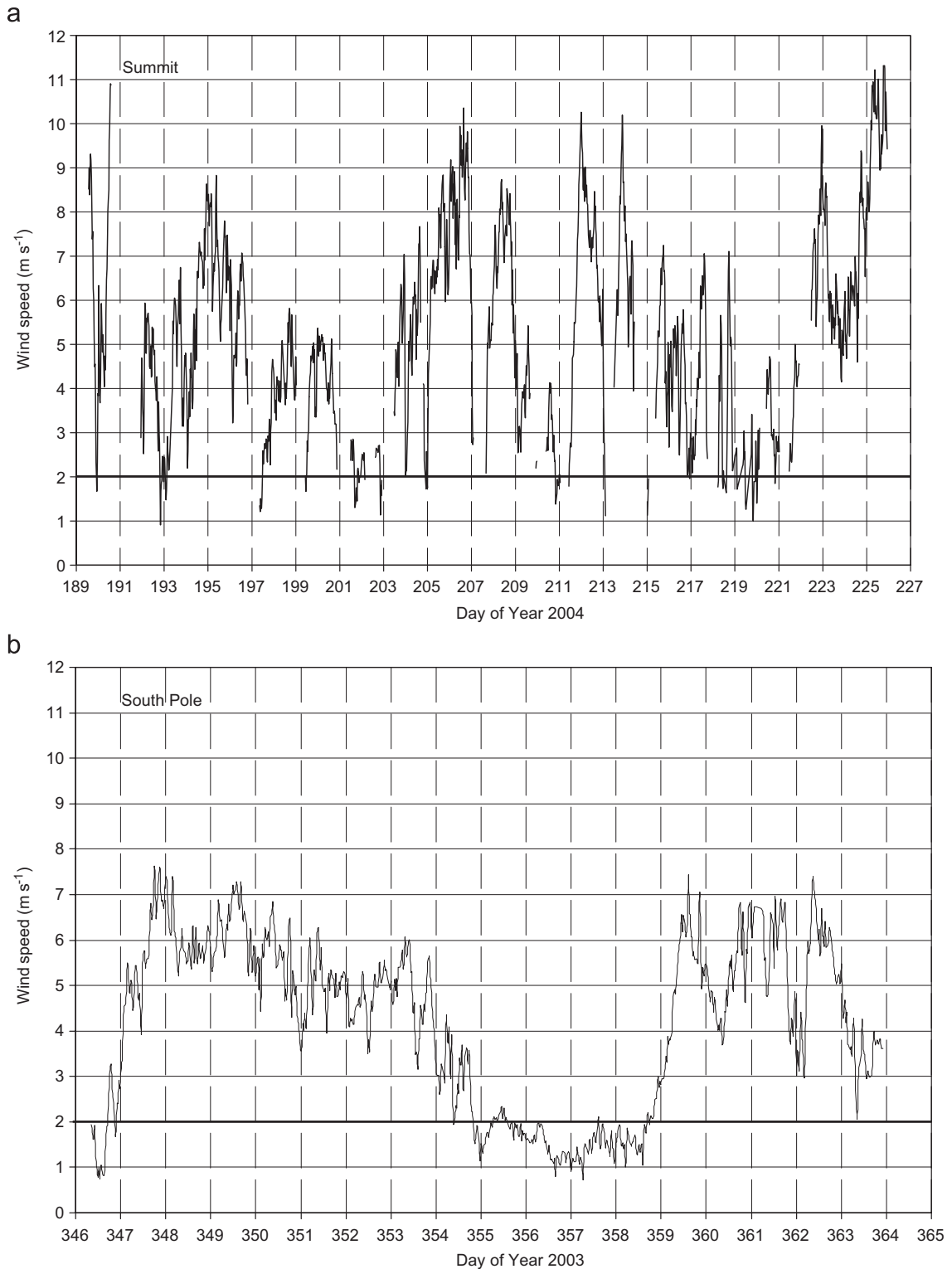


Fig. 4. Summertime wind speeds at Summit (upper graph, a) and South Pole (lower graph, b) derived from sonic anemometer data at 2 m. The Summit data are from DOY 189–226, 2004 (July 8–August 14); South Pole data are from DOY 346–364, 2003 (December 12–30).

Table 2
Duration of calm wind conditions ($\leq 2 \text{ m s}^{-1}$) for Summit and South Pole experiments

	Duration of calm winds				Total percentage of calm winds
	1–5 h	6–10 h	11–15 h	15+ h	
Summit March–April 2005 (39 days)	44%	17%	33%	6%	18%
Summit July–August 2004 (36 days)	54%	27%	19%	0%	22%
South Pole December 2003 (18 days)	0%	67%	0%	33%	22%

Percentages are based on half-hour resolution turbulence data and meteorological data.

(z/L) whose sign mirrors the sign of the surface heat flux. Prior to week 16 (22–28 April), when the average daily heat fluxes are always negative, surface layer conditions are always weakly to strongly stable (z/L positive). During the summer weeks, the surface layer becomes unstable (z/L negative) during the daytime between 0900 and 1900 h GMT (0700–1700 h local time).

Unstable conditions characterize 9.8% of the March–April 2005 observations and 51% of the July–August 2004 observations. Although objective filtering of the turbulence data for contamination or instrument failure biases the observations against strongly stable cases (very cold temperatures and rime events) the evident difference in surface layer conditions between the seasons is of note. Similar surface layer conditions were reported by Cullen and Steffen (2001), who describe unstable conditions occurring at Summit 38% of the time during June–July 2000. These researchers also showed that, for the entire Greenland ice sheet, unstable conditions occurred 43%, 14% and 11% during the summer months for 1998, 1999, and 2000, respectively, based on gradient Richardson number calculations. Helmig et al. (2002) also report unstable conditions (based on gradient Richardson number) occurring daily between 0900 and 1600 h (LST) during June 2000. Schelander et al. (2003) report weak unstable stratification during the summer (June–August) occurring 21% of the time, but that during winter months (December–February) boundary layer conditions were always stably stratified.

A characteristic feature in the boundary layer structure at Summit is the frequent presence of wind speed maxima at the top of the boundary layer height. This feature is clearly visible in Fig. 9, where 3 weeks of tethered balloon vertical profile data and continuous wind speed observations from an automated weather station (at 2 m) were combined in a color contour plot for illustration of the temporal and vertical distribution of wind speed over the

Summit camp (further details on the tethered balloon experiment and the data analysis have been presented in detail elsewhere (Helmig et al., 2002, 2007b)). During most days with stronger winds, the maximum wind speed was observed between 50 and 300 m height above the ground. This analysis also shows a diurnal cycle in wind speed during most days, with wind speed maxima typically occurring during the later part of the day. These wind speed data in addition to wind direction and potential temperature profile data were used to calculate the distribution of atmospheric stability based on the gradient Richardson number. This analysis showed a vertically inhomogeneous distribution of atmospheric stability with many stable and unstable sublayers between the surface and 500 m above the snow surface. The same analysis was done for a December 2003 data set from the South Pole. These data showed a much more homogenous distribution of stability, with stable atmospheric conditions between the snow surface and 500 m. Furthermore, the temporal changes were less frequent and on several occasions, such stable atmospheric conditions were sustained for several days (Neff et al., 2007). As described by Neff et al. (2007) for the South Pole, the possibility of non-linear chemistry affecting NO in the boundary layer depends on both the mixing layer depth and the rate of diffusion from the surface into the mixing layer: A slow rate of upward diffusion can reduce the effective mixing layer depth vis-à-vis that measured using sodars or other conventional methods. Fig. 10 shows the Summit spring 2005 time series of eddy diffusion times for a boundary depth of 25 m. Based on Brost and Wyngaard (1978), this diffusion time was estimated from scale analysis as

$$T_D = h^2 / K_M, \quad (4)$$

where h is the boundary layer depth. The eddy diffusion coefficient K_M , was calculated assuming

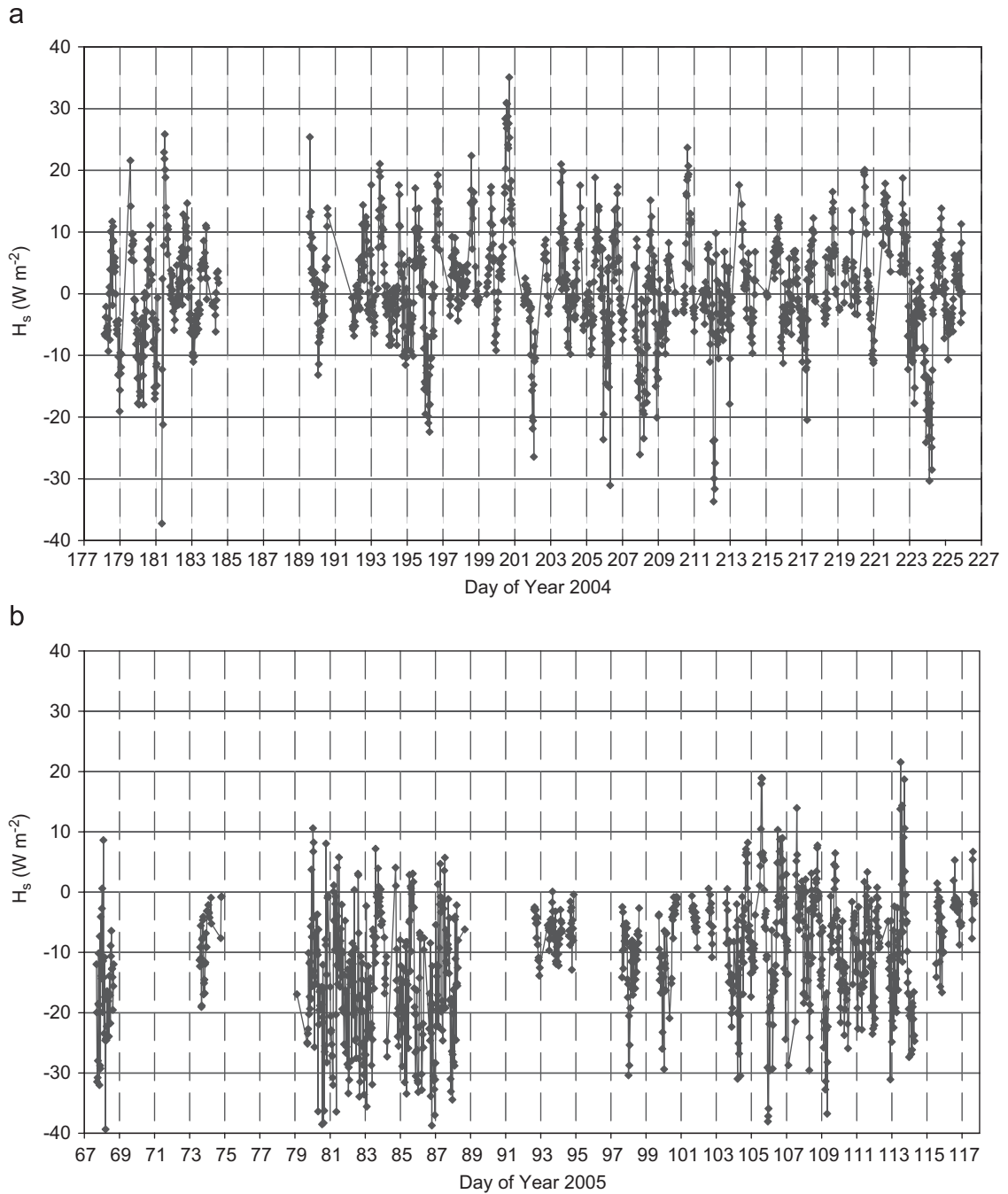


Fig. 5. Sensible heat fluxes at Summit during July–August 2004 (DOY 178–226) (upper graph, a) and March–April 2005 (DOY 68–117) (lower graph, b).

a turbulent Prandtl number of order unity ($K_M \sim K_H$) from turbulence data and temperature gradients in the surface layer using

$$\overline{w'\theta'} = -K_H \frac{\partial \theta}{\partial z}. \tag{5}$$

High eddy diffusion times ($T_D > 100$ min) indicate very slow turbulent mixing, which will strongly affect surface layer chemistry. As seen in Fig. 10, these conditions occurred several times during the spring observation period for an average duration of 3.5 h. Slow diffusion times also occurred during

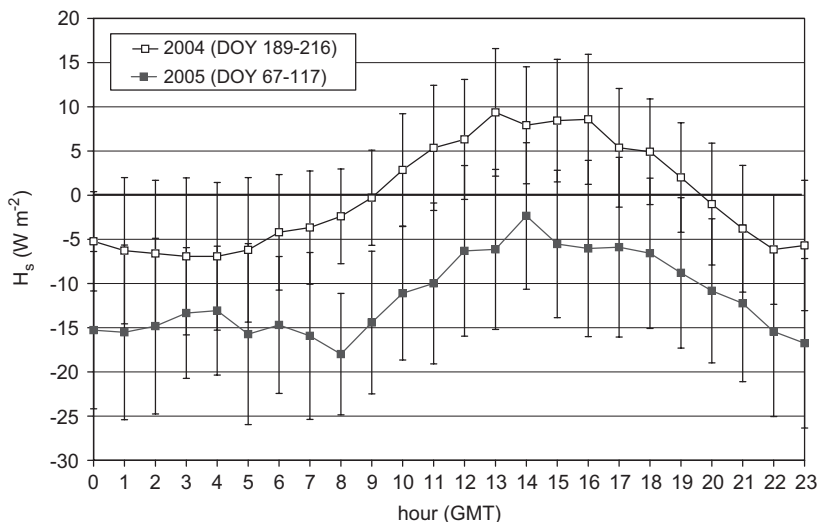


Fig. 6. Diurnal cycle of sensible heat flux averaged over the entire summer 2004 and spring 2005 observation periods. Error bars are 1 standard deviation.

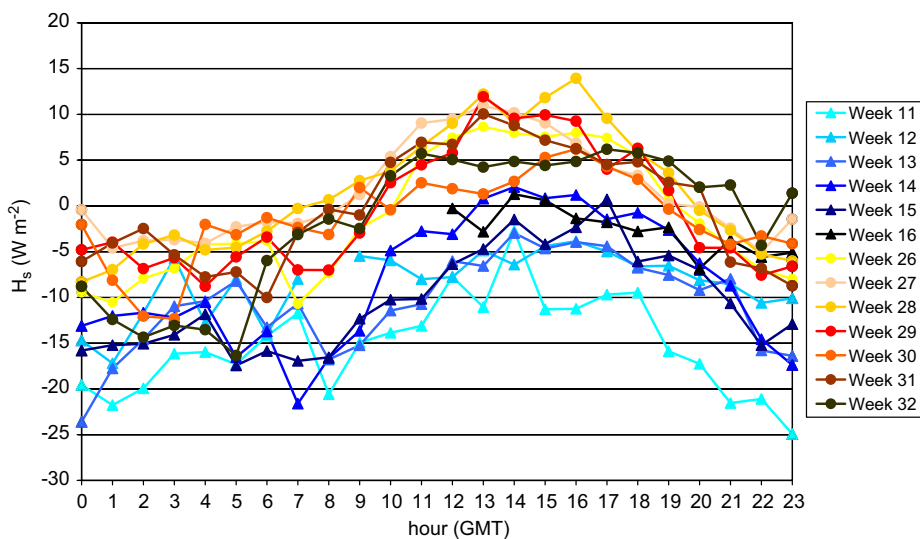


Fig. 7. Diurnal cycles of sensible heat flux averaged weekly. Weeks 11–16 constitute the 2005 observations (March 22–April 27); Weeks 26–32 (June 27–August 13) constitute the 2004 season. Note positive heat fluxes between ~0900 and 2000 h for the summer weeks.

summer months at Summit and lasted for up to 11 h on two occasions. In contrast, at South Pole, Neff et al. (2007) found periods greater than 3 days for similar eddy diffusion times, implying vastly different time scales for surface layer chemistry to occur at South Pole than at Summit.

3.4. Boundary layer heights

In contrast to mid-latitude boundary layer development where heat flux (convection) drives the

boundary layer growth during the daytime, in the Arctic heat fluxes are negative for much of the year and small even in the summer. In these cases, wind-shear induced mixing is the driving force for the growth of the boundary layer into the overlying statically stable atmosphere. Neff (1980) estimated boundary layer heights at South Pole using a diagnostic mixed-layer formulation developed originally for the stable oceanic mixed layer (Pollard et al., 1973) and tested these results with sodar and surface flux estimations that used MO similarity.

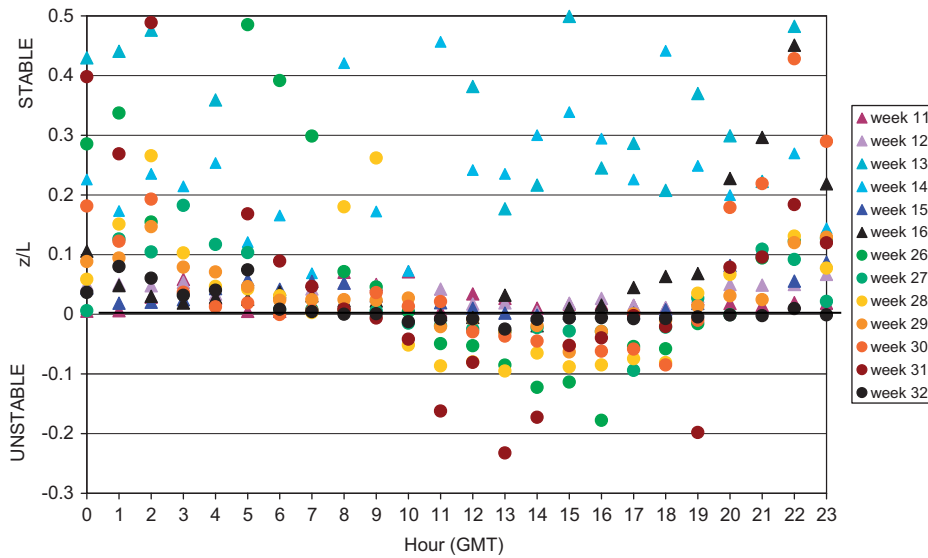


Fig. 8. Diurnal cycle of stability parameter z/L averaged weekly as in Fig. 7.

Scaling expressions using the surface heat flux proved problematic because of changes in the surface radiative budget that were rapid compared to the evolution of the boundary layer height. For these reasons, the equation used for determining the boundary-layer height (for equilibrium conditions) in the current analysis is given by

$$h = 1.2u_*(fN)^{-1/2}, \tag{6}$$

where N is the Brunt–Vaisala frequency, and f is the Coriolis parameter. The numerical constant was modified from that of Pollard et al. for a critical Richardson number of 0.25 rather than 1.0. The Brunt–Vaisala frequency is a measure of the stability in a statically stable surface layer. It is calculated using the sonic-derived virtual temperature, T_v , and the potential temperature gradient over 2–0.75 m using the following equation (Stull, 1988),

$$N = \left(\frac{g}{T_v} \frac{\partial \theta}{\partial z} \right)^{1/2}. \tag{7}$$

This model for determining boundary-layer height was successfully compared with estimates of boundary layer height from sodar measurements at South Pole under weak-to-moderate stability cases and for heights in excess of 50 m (Neff, 1980). For recent South Pole observations (Neff et al., 2007), this method (tested with both tower finite differences as well as rawinsonde temperature profiles)

worked well for very stable conditions ($h < 50$ m) but underestimated the mixing layer depth for deeper mixing layers ($h > 100$ m). Because the method depends on the fourth root of the vertical temperature gradient, the result is more sensitive to the surface stress u_* .

Boundary layer heights were calculated using Eq. (6) for conditions when convection is zero or very weak ($z/L > -0.1$), that is, when the mixing is dominated by the wind and not the heating of the surface and the overlying atmosphere is statically stable (Figs. 11a and b). The primary scaling parameter u_* , is also plotted. Aside from the overall variation with wind speed (friction velocity), a diurnal cycle can be seen for both data sets, where boundary layer heights are lowest during the night and reach their peaks during the daytime. In addition, several consecutive days of low boundary layer heights (< 100 m) occurred during the spring observation period, but this sustained stability was not seen during the summer.

Unfortunately, unlike during the ANTCI program at the South Pole, there were no extensive direct measurements of the mixing layer such as those using sodars or tethered balloons. However, four ozonesondes that were launched during spring 2005 can be used as test cases to compare direct observation of the boundary layer height with the values calculated from the surface turbulence parameters. These four ozonesonde launches are the only ones during the 2005 experiment which

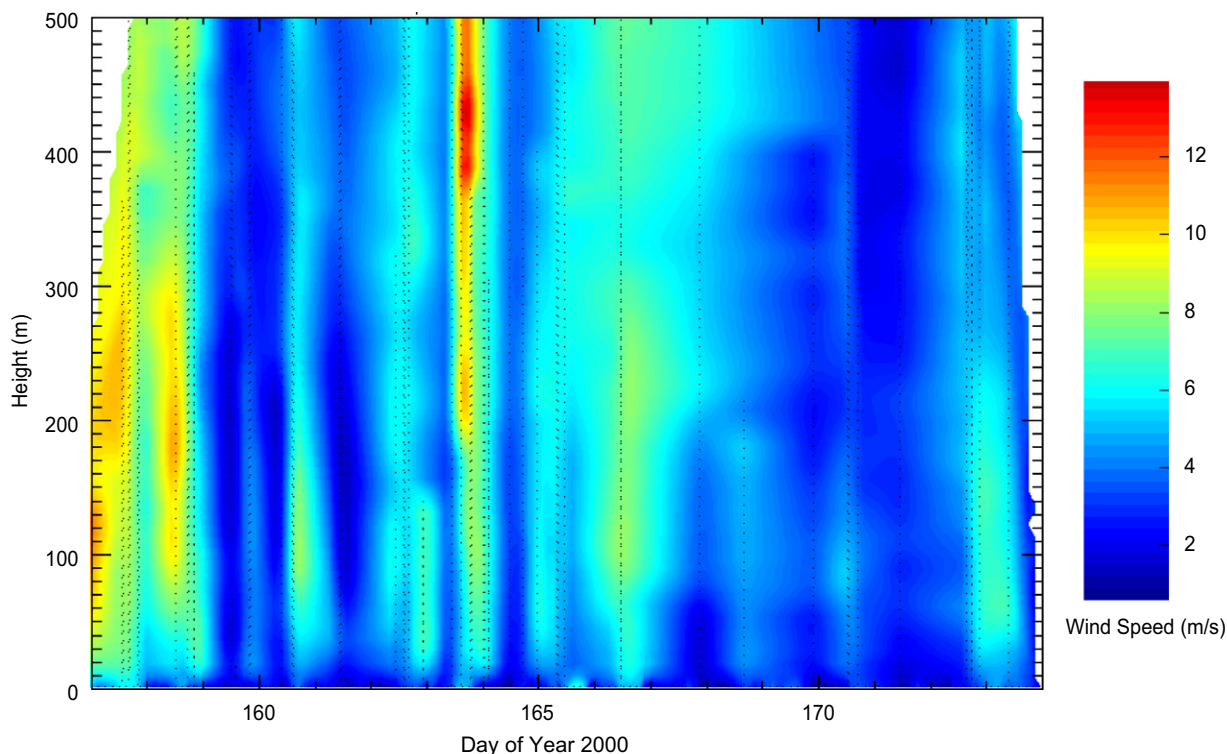


Fig. 9. Vertical and temporal structure of wind speed over Summit during the summer of 2000. These data were collected during tethered balloon profiles and from an automated weather station during June 3–21, 2000. The distribution of data that went into this interpolation is indicated by black dots.

were concurrent with sonic anemometer data. Boundary layer heights were estimated as the height of the temperature inversion from the rawinsonde profiles (in accordance to stable boundary layer height evaluations suggested by Vickers and Mahrt, 2004). These temperature profiles are shown in Fig. 12, and their corresponding half-hour boundary layer heights calculated from turbulence data are summarized in Table 3.

Previous estimations of boundary layer heights for Summit using the profile of temperature or potential temperature from rawinsondes offer similar values. Schelander et al. (2003) observed a mean boundary layer height of 210 m during the winter (December–February), while the Helmig et al. (2002) measurements in June report diurnal cycles of boundary layer heights between ~70 and 250 m during the daytime and zero or near-zero at nighttime.

Because we lack extensive validation of boundary layer heights during our observation periods, the calculated boundary layer height values must be carefully applied. The Monin–Obukhov similarity

theory, which underlies all assumptions in applying surface layer (2 m a.g.) turbulence data to describing the atmospheric boundary layer, works well in neutral to weakly stable ($0 < z/L < 0.1–0.4$) atmospheric conditions, but it seems that the similarity theory is less useful for very stable cases (Forrer and Rotach, 1997; Grachev et al., 2005). In addition, we have not calculated boundary layer heights for strongly unstable (convective) conditions during the summer observation period. Studies at South Pole have calculated boundary layer heights for unstable cases based on the integral length scales of the turbulence data (Onclay et al., 2004).

Given that Summit boundary layer conditions are in large part influenced by the cycle of diurnal solar radiation, we did not observe the extended periods of stable conditions that characterize South Pole. While diurnal stability cycles (stable at night, weakly stable to weakly unstable during the day) are readily seen throughout the spring and summer at Summit, South Pole boundary layer conditions often become very stable on large temporal and spatial scales.

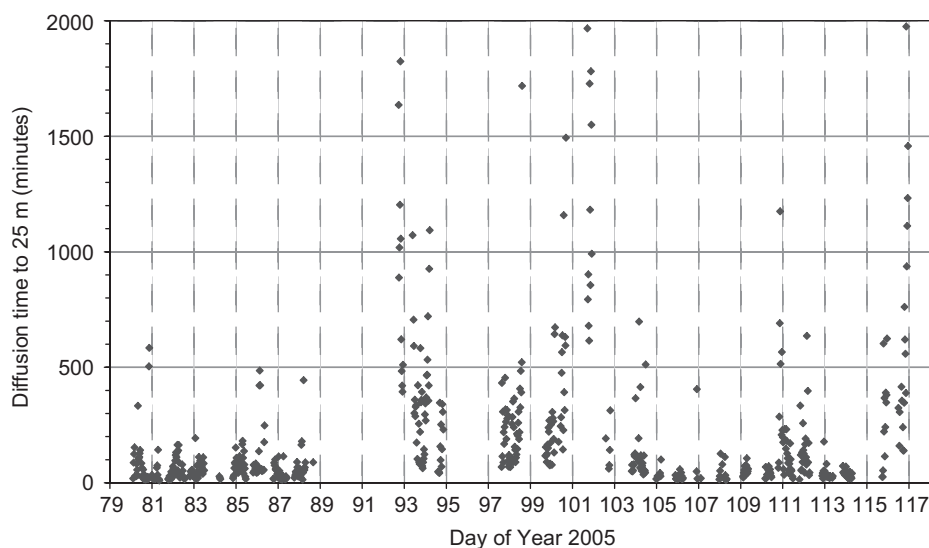


Fig. 10. Eddy diffusion times for a 25 m boundary layer height at Summit (March–April 2005). Slow upward diffusion times (> 100 min) often occur, but only persist for 1–8 h.

A diurnal evolution of the boundary layer height during the summer (reaching elevations of 250–400 m during the daytime) was also reported by [Argentini et al. \(2005\)](#) at Dome C, Antarctica from analysis of sonic anemometer and sodar data. The Dome C site is quite similar to Summit in meteorology (temperatures between -40 and -20 °C, mean wind speed 4.8 m s^{-1}), solar radiation (latitude 74°S) and topography (snow-covered surface with near-zero slope on the Antarctic plateau at 3233 m above sea level).

An important question for surface layer chemistry is for how long and in what volume can snowpack emissions accumulate in the surface layer. The depth and temporal variations of the mixed layer were addressed in the previous sections. The significant differences in the topography and snowpack residence times between Summit and South Pole must also be examined. In contrast to South Pole, Summit is at the topographic high point of the surrounding ice sheet ([Fig. 1](#)). Slopes comparable to those surrounding South Pole (1 part in 1000) extend from Summit a maximum of ~ 400 km. South Pole, however, is not at a topographic high, and boundary-layer air flowing over the South Pole typically drains from the Antarctic plateau over a fetch on the order of 1000 km. Thus for very stable conditions with weak winds, conditions for which the boundary layer is quite shallow, the footprint of surrounding snowpack over which air is advected is significantly smaller for Summit than for South Pole.

4. Conclusions

A number of conditions and processes were identified that define the ventilation of the Summit surface layer, the residence time of snowpack emissions near the surface and their possible influence and contribution to atmosphere reaction cycles. Differences in the Summit and South Pole surface layer chemistry that were pointed out in several previous investigations ([Davis et al., 2004](#); [Helmig et al., 2007d](#)) can be attributed to a large extent to different boundary layer dynamics and the much longer fetch for winds at the South Pole from the high Antarctic plateau.

The surface and boundary layer at Summit is influenced by diurnal, summertime radiation cycles. Diurnal heat flux cycles contribute towards daytime boundary layer growth and a diurnal cycle of surface and boundary layer mixing that provides for regular ventilation of the surface layer. At South Pole, which lacks a diurnal radiation cycle and has overall smaller sensible heat fluxes, ventilation of the surface layer is more dependent on synoptic transport conditions, and wind speeds in excess of $3\text{--}5 \text{ m s}^{-1}$ are required for a breakup of stable, stratified surface layer conditions. Sustained summertime stable surface layer conditions as reported for South Pole, were not evident in the Summit observations.

Secondly, the fetch and residence/transport time over snow surface for boundary layer winds at Summit is

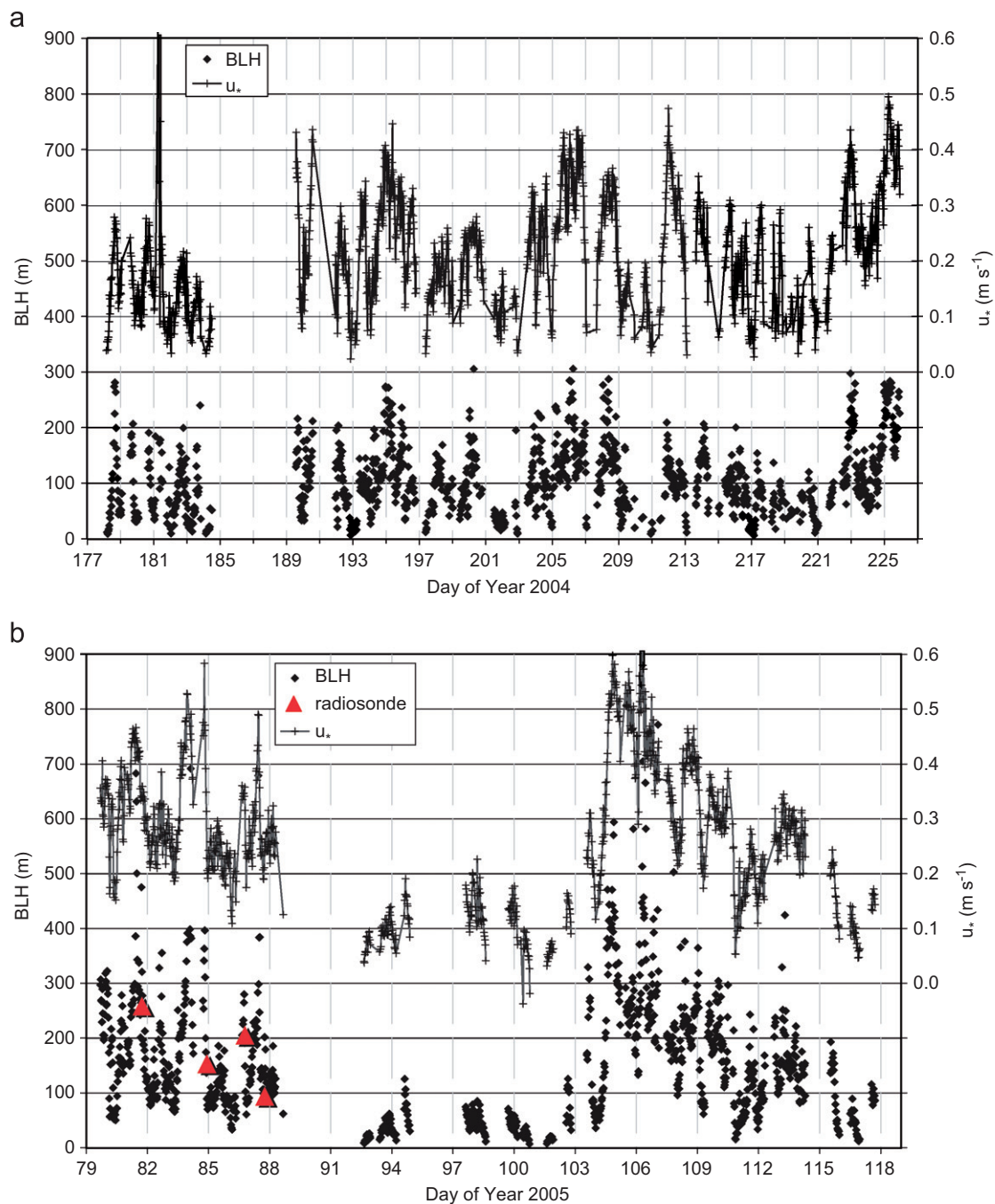


Fig. 11. (a and b) Boundary layer heights and friction velocity (u_*) for summer 2004 (upper graph) and spring 2005 (lower graph). Friction velocity (u_*) is the primary scaling parameter for boundary layer height using equation (6). The four radiosonde-derived boundary layer heights are shown for comparison in (b). Boundary layer heights are only calculated for weakly unstable to stable surface layer conditions.

much shorter than at South Pole. Given the increased ventilation and the lower transport/residence time over the snowpack, shorter accumulation times of gases emitted from the sunlit snowpack are expected at

Summit. This suggestion is in agreement with available information on gas concentrations at these two sites. Furthermore, oxidation chemistry that is dependent on atmospheric levels of snowpack emissions is expected

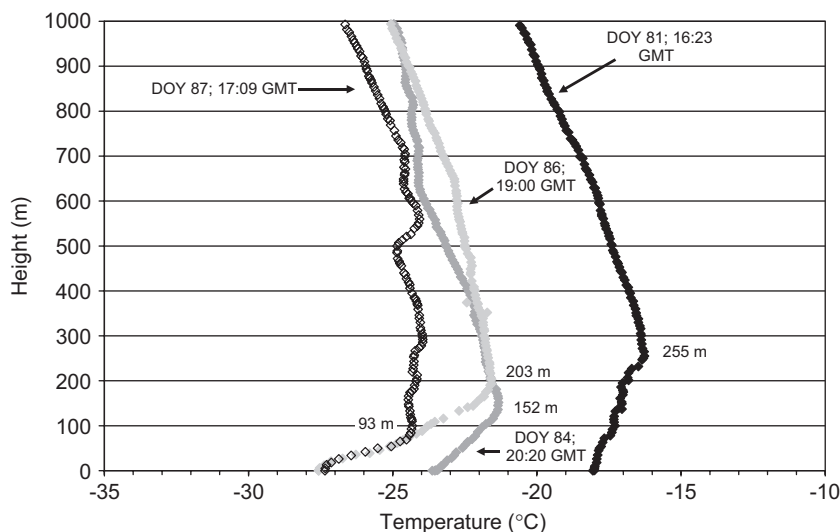


Fig. 12. Radiosonde temperature profiles and estimated boundary layer heights from four balloon launches during spring 2005 (data courtesy NOAA GMD).

Table 3

Boundary layer height estimates from radiosonde data and from surface layer turbulence data

Radiosonde BLH estimation		Turbulence BLH estimation	
DOY 81; 16:23 GMT	255 m	DOY 81; 16:00–16:30 GMT	264 m
DOY 84; 20:20 GMT	152 m	DOY 84; 20:00–20:30 GMT	200 m
DOY 86; 19:00 GMT	203 m	DOY 86; 18:30–19:00 GMT	149 m
DOY 87; 17:09 GMT	93 m	DOY 87; 17:00–17:30 GMT	129 m

to be weaker at Summit, due to the expected lower atmospheric levels of precursor compounds.

Acknowledgements

We would like to thank the ETH (Swiss Federal Institute of Technology, Institute for Atmospheric and Climate Science) for readily providing meteorological data and also the NOAA GMD for providing radiosonde data. K. Steffen and N. Cullen, University of Colorado, Boulder, provided advice in the experiment planning, data analysis, valuable comments on a draft manuscript, the AWS surface data, and Fig. 1. T. Morse, University of Colorado, Boulder analyzed data that are displayed in Fig. 9. S. Oncley, National Center for Atmospheric Research, Boulder, Colorado provided invaluable help in the evaluation of the sonic anemometer for the 2004 measurements. Logistical support was provided by VECO Polar Resources and the US 109th Air National Guard.

We also thank the Danish Commission for Scientific Research for providing access to the Summit research site. This research was funded by the United States National Science Foundation (Office of Polar Programs #0240976). Any opinions, findings, and conclusions expressed in this material are those of the authors and do not necessarily reflect the views of the National Science Foundation.

References

- Albert, M.R., Hawley, R.L., 2000. Seasonal differences in surface energy exchange and accumulation at Summit, Greenland. *Annals of Glaciology* 31, 387–390.
- Andreas, E.L., Cash, B.A., 1996. A new formulation for the Bowen ratio over saturated surfaces. *Journal of Applied Meteorology* 35, 1279–1289.
- Argentini, S., Viola, A., Sempreviva, A.M., Petenko, I., 2005. Summer boundary-layer height at the plateau site of dome C, Antarctica. *Boundary-Layer Meteorology* 115, 409–422.
- Bottenheim, J.W., Dibb, J.E., Honrath, R.E., Shepson, P.B., 2002. An introduction to the ALERT 2000 and SUMMIT

- 2000 Arctic research studies. *Atmospheric Environment* 36, 2467–2469.
- Brost, R.A., Wyngaard, J.C., 1978. A model study of stably stratified planetary boundary-layer. *Journal of the Atmospheric Sciences* 35, 1427–1440.
- Crawford, J.H., Davis, D.D., Chen, G., Buhr, M., Oltmans, S., Weller, R., Mauldin, L., Eisele, F., Shetter, R., Lefer, B., Arimoto, R., Hogan, A., 2001. Evidence for photochemical production of ozone at the South Pole surface. *Geophysical Research Letters* 28, 3641–3644.
- Cullen, N.J., 2003. Characteristics of the atmospheric boundary layer at Summit, Greenland. Ph.D. Thesis, University of Colorado, Boulder, 146pp.
- Cullen, N.J., Steffen, K., 2001. Unstable near-surface boundary conditions in summer on top of the Greenland ice sheet. *Geophysical Research Letters* 28, 4491–4493.
- Davis, D., Nowak, J.B., Chen, G., Buhr, M., Arimoto, R., Hogan, A., Eisele, F., Mauldin, L., Tanner, D., Shetter, R., Lefer, B., McMurry, P., 2001. Unexpected high levels of NO observed at South Pole. *Geophysical Research Letters* 28, 3625–3628.
- Davis, D., Chen, G., Buhr, M., Crawford, J., Lenschow, D., Lefer, B., Shetter, R., Eisele, F., Mauldin, L., Hogan, A., 2004. South Pole NO_x chemistry: an assessment of factors controlling variability and absolute levels. *Atmospheric Environment* 38, 5375–5388.
- Forrer, J., Rotach, M.W., 1997. On the turbulence structure in the stable boundary layer over the Greenland ice sheet. *Boundary-Layer Meteorology* 85, 111–136.
- Grachev, A.A., Fairall, C.W., Persson, P.O.G., Andreas, E.L., Guest, P.S., 2005. Stable boundary-layer scaling regimes: the SHEBA data. *Boundary-Layer Meteorology* 116, 201–235.
- Helmig, D., Boulter, J., David, D., Birks, J.W., Cullen, N.J., Steffen, K., Johnson, B.J., Oltmans, S.J., 2002. Ozone and meteorological boundary-layer conditions at Summit, Greenland, during 3–12 June 2000. *Atmospheric Environment* 36, 2595–2608.
- Helmig, D., Oltmans, S.J., Carlson, D., Lamarque, J.F., Jones, A., Labuschagne, C., Anlauf, K., Hayden, K., 2007a. A review of surface ozone in the polar regions. *Atmospheric Environment*, this issue, [10.1016/j.atmosenv.2006.09.053](https://doi.org/10.1016/j.atmosenv.2006.09.053).
- Helmig, D., Oltmans, S.J., Morse, T.O., Dibb, J.E., 2007b. What is causing high ozone at Summit, Greenland? *Atmospheric Environment*, this issue, [10.1016/j.atmosenv.2006.05.084](https://doi.org/10.1016/j.atmosenv.2006.05.084).
- Helmig, D., Bocquet, F., Cohen, L., Oltmans, S.J., 2007c. Ozone uptake to the polar snowpack at Summit, Greenland. *Atmospheric Environment*, this issue, [10.1016/j.atmosenv.2006.06.064](https://doi.org/10.1016/j.atmosenv.2006.06.064).
- Helmig, D., Johnson, B., Oltmans, S.J., Neff, W., Eisele, F., Davis, D.D., 2007d. Elevated ozone in the boundary layer at South Pole. *Atmospheric Environment*, in press, [10.1016/j.atmosenv.2006.12.032](https://doi.org/10.1016/j.atmosenv.2006.12.032).
- Honrath, R.E., Yu, Y., Peterson, M.C., Dibb, J.E., Arsenault, M.A., Cullen, N.J., Steffen, K., 2002. Vertical fluxes of NO_x, HONO, and HNO₃ above the snowpack at Summit, Greenland. *Atmospheric Environment* 36, 2629–2640.
- Kaimal, J.C., Finnigan, J.J., 1994. *Atmospheric Boundary Layer Flows: Their Structure and Measurements*. Oxford University Press, New York, Oxford, 289pp.
- Kaimal, J.C., Gaynor, J.E., 1991. Another look at sonic thermometry. *Boundary-Layer Meteorology* 56, 401–410.
- Larsen, S.E., Edson, J.B., Fairall, C.W., Mestayer, P.G., 1993. Measurement of temperature spectra by a sonic anemometer. *Journal of Atmospheric and Oceanic Technology* 10, 345–354.
- Mauldin III, R.L., Kosciuch, E., Henry, B., Eisele, F.L., Shetter, R., Lefer, B., Chen, G., Davis, D., Huey, G., Tanner, D., 2004. Measurements of OH, HO₂ + RO₂, H₂SO₄, and MSA at the South Pole during ISCAT 2000. *Atmospheric Environment* 38, 5423–5437.
- Neff, W. D., 1980. An observational and numerical study of the atmospheric boundary layer overlying the east Antarctic ice sheet. Ph.D. Thesis, Department of Astrogeophysics, University of Colorado, 272pp.
- Neff, W.D., Helmig, D., Grachev, A., Davis, D., 2007. A study of boundary layer behavior associated with high surface NO concentrations at the South Pole using a minisodar, tethered balloon, and sonic anemometer. *Atmospheric Environment*, in press, [10.1016/j.atmosenv.2007.01.033](https://doi.org/10.1016/j.atmosenv.2007.01.033).
- Oltmans, S.J., Johnson, B.J., Helmig, D., 2007. Episodes of high surface ozone amounts at South Pole during summer and their impact on the long-term surface ozone variation. *Atmospheric Environment*, in press, [10.1016/j.atmosenv.2007.01.020](https://doi.org/10.1016/j.atmosenv.2007.01.020).
- Oncley, S.P., Buhr, M., Lenschow, D.H., Davis, D., Semmer, S.R., 2004. Observations of summertime NO fluxes and boundary-layer height at the South Pole during ISCAT 2000 using scalar similarity. *Atmospheric Environment* 38, 5389–5398.
- Pollard, R.T., Rhines, P.B., Thompson, R.O.R.Y., 1973. The deepening of the wind-mixed layer. *Geophysical Fluid Dynamics* 3, 381–404.
- Schelander, P., Ohmura, A., Calanca, P., 2003. Seasonal variability of the boundary layer structure at Summit, Greenland. *JSM16/O4A/C31-003*, IUGG, Sapporo, Japan.
- Stearns, C.R., Weidner, G.A., Keller, L.M., 1997. Atmospheric circulation around the Greenland crest. *Journal of Geophysical Research* 102, 13801–13812.
- Steffen, K., Box, J.E., 2001. Surface climatology of the Greenland ice sheet: Greenland Climate Network 1995–1999. *Journal of Geophysical Research* 106, 33951–33964.
- Stull, R.B., 1988. *An Introduction to Boundary Layer Meteorology*. Kluwer Academic Publishers, Dordrecht, 666pp.
- Vickers, D., Mahrt, L., 2004. Evaluating formulations of stable boundary layer height. *Journal of Applied Meteorology* 43, 1736–1749.